



Mechanism studies on thermal dissociation of tri-*n*-octylamine hydrochloride with FTIR, TG, DSC and quantum chemical methods

CHUNHUA DONG^{a,b}, XINGFU SONG^{a,*} , EVERT JAN MEIJER^b, GUILAN CHEN^a,
YANXIA XU^a and JIANGUO YU^{a,*}

^aNational Engineering Research Center for Integrated Utilization of Salt Lake Resource, East China University of Science and Technology, Meilong Road 130, Shanghai 200237, China

^bVan 't Hoff Institute for Molecular Sciences & Amsterdam Center for Multiscale Modeling, University of Amsterdam, 1098 XH Amsterdam, The Netherlands
E-mail: xfsong@ecust.edu.cn; jgyu@ecust.edu.cn

MS received 26 May 2017; revised 11 July 2017; accepted 23 July 2017; published online 2 September 2017

Abstract. The thermal dissociation of tri-*n*-octylamine hydrochloride (TOAHCl) was investigated using both the quantum chemical simulation and experimental methods. The pathway through which a mixture of tri-*n*-octylamine (TOA) and hydrogen chloride (HCl), rather than di-*n*-octylamine (DOA) and 1-chlorooctane, are produced has been determined through transition state (TS) search with Intrinsic Reaction Coordinate (IRC) calculations. Particularly, strong agreement between the experimental FTIR spectra and that of TOA demonstrates the same result for the first time. Moreover, the thermal dissociation of TOAHCl proceeds in two continuous steps, which is different from the low molecular mass amine hydrochlorides. The experimental enthalpy of the dissociation was 70.793 kJ mol⁻¹ with DSC measurement which is very close to the density functional theory (DFT) calculation result 69.395 kJ mol⁻¹. Furthermore, with the aid of DFT calculations, some other important thermochemical characteristics such as crystal lattice energy with the value of 510.597 kJ mol⁻¹ were evaluated by means of Born–Fajans–Haber cycle.

Keywords. Tri-*n*-octylamine hydrochloride; TG-FTIR; DSC; thermal dissociation mechanisms; intrinsic reaction coordinate.

1. Introduction

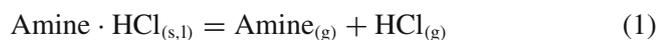
As effective extractants, high molecular mass aliphatic water-insoluble amines, especially tertiary amines such as tri-*n*-octylamine (TOA), tris-(2-ethylhexyl)-amine (TEHA), N235 (a mixture of tertiary amines with carbon number 8 to 10 in each chain), are used for the extraction of HCl directly from HCl-containing solutions^{1–9} or in the reactive extraction–crystallization coupled process of CaCl₂,^{10–13} MgCl₂,^{13,14} SrCl₂,¹⁵ LiCl,¹⁶ etc. (converting them to their respective carbonates by introducing CO₂ and amine extractants, such as TOA). Systematic work has been done for CaCl₂^{10,11} and MgCl₂¹⁴ in our group which could release the stress of dealing with the high CaCl₂-containing (90–120 g L⁻¹) distiller waste derived from ammonia-soda process and the high MgCl₂-containing (mass fraction >30%) brines after

production of potassium fertilizers from Qinghai Salt Lake, respectively. Apart from tackling waste solutions, it is a promising way to keep CO₂ in storage. Fortunately, both the conversion rate and yield are high enough to bring about industrialization. However, how to regenerate the expensive extractants effectively is the key to realizing the aim. Many alternative ways, which are more effective and easier, such as using lime slurry, ammonia solutions and other alkaline substances (e.g., NaOH) could be chosen to regenerate the amine extractants.^{1,17–19} However, all these methods result in other substances which are of very low value or are considered as wastes and considerable purchase costs of such alkaline substances should be taken into account. Some researches on stripping HCl with distilled water have been done, which showed high efficiency for TEHA, but less than 10% for TOA and others.^{6–8,20,21} By comparison, thermal dissociation of amine hydrochlorides

*For correspondence

is a promising technique of zero emission for resource utilization that could regenerate extractants as well as produce largely attractive gaseous HCl.^{22–27} A pilot plant where TEHA is used to recycle HCl by applying thermal dissociation approach in the process of making ethanol from biomass has been built.^{26,27}

Much work has been done mainly by Jerzy Błazejowski, for the mechanism of thermal dissociation of amine hydrochlorides (including NH_4Cl) which could be expressed by the general formula $[\text{C}_n\text{H}_{2n+1}\text{NH}_3]\text{Cl}$, with $n = 0 - 8$ ^{28–31} and $[(\text{C}_n\text{H}_{2n+1})_p\text{NH}_{4-p}]\text{Cl}$, with $n = 1-4$, $p = 2-4$.^{32–35} Irrespective of the chain-length, the thermal dissociation of amine hydrochlorides occurs in one step just as NH_4Cl does, which could be expressed by equation:



It was reported that dissociation of amine hydrochlorides mentioned above proceeded and nearly reached the boiling points of the corresponding amines. The amine should thus appear along with HCl in the gas phase.^{28,29,32} In Jerzy Błazejowski's work, TG/DTG/DTA curves of tertiary amine hydrochlorides were drawn, indicating that there is only one endothermic peak. Unlike the amine hydrochlorides mentioned above, the thermal dissociation process of TOAHCl was somewhat different due to TOA's high boiling point (365.8°C), which is over 150°C higher than the dissociation temperature.

To find out the mechanism of thermal dissociation of high molecular mass amine hydrochloride, whose boiling point of the corresponding amine is much higher than the dissociation temperature, is the primary target in this paper. Thus we try to study the two possible pathways of dissociation theoretically with DFT calculations to find the dominant one. Besides, this work will provide basic data for thermal dissociation of TOAHCl to help to realize the industrialization of the reactive extraction–crystallization coupled process of all kinds of metal chloride wastes.

2. Computational and Experimental details

2.1 Intrinsic reaction coordinate (IRC) calculations

The nudged elastic band (NEB) method^{36,37} is a technique through which the minimum energy path of a certain process can be studied. Offering at least the reactants and products coordinates, a band of images could be constructed and their energy perpendicular to the band could be then minimized. Along the band, the images are connected through springs. Convergence of this method leads to the minimum energy path (MEP). Specifically, climbed images nudged elastic band

(CI-NEB) method was used to get a rough transition state (TS) structure. All the calculations were carried out on CP2K package.³⁸ Then the fine TS structure was optimized through TS (Berny) method at B3LYP/6-31+G(d, p) level firstly and then at B3LYP/6-311++G(d, p) level. Afterwards, it was approved by frequency calculation-with only one imaginary frequency on the reaction pathway. Finally, it was confirmed by IRC calculations. The energy barriers could be calculated after the confirmation of pathways. The reactant and products were optimized at the level of B3LYP/6-311++G(d, p) to calculate the thermal related parameters. These calculations were carried out with Gaussian 09 software package.³⁹ Some important calculation details are shown in Supplementary Information.

2.2 Materials

Analytical reagent TOA (purity $\geq 97.0\%$) was purchased from TCI (Shanghai) Development Co., Ltd., Shanghai, China. Petroleum ether (boiling range, 60–90°C), hydrochloric acid of analytical grade were purchased from Shanghai Ling Feng Chemical Reagent Co. Ltd., Shanghai, China.

2.3 Preparation of TOAHCl

TOAHCl was obtained by dissolving 0.1 mol (about 35.4 g) of TOA in 40–60 mL cold petroleum ether (in the jacketed reactor, isopropanol-water mixed solutions as the cooling medium) and adding 0.11–0.12 mol of concentrated HCl solutions (9–10 mL) slowly in case of quick temperature increase. Although a white precipitate formed immediately, it was necessary to keep the solution at about 0°C for at least 1 h to achieve a high yield. Transparent flakes were gathered after three times of recrystallization from warm petroleum ether. Then the salts were filtrated using Buchner funnel, washing with ice-cold petroleum ether and dried overnight in vacuum at room temperature firstly, then at 50°C in order to release the remaining petroleum ether. Then TOAHCl crystals were obtained.

2.4 Characterization

Purity was checked by elementary analysis which was conducted with Elementar vario EL III elemental analyzer (Elementar Analysensysteme GmbH, Germany). The elementary analysis results are shown in Table 1.

The thermal dissociation mechanism of TOAHCl was analyzed by comparing FTIR spectrum of TOA (liquid film method) with that of TOAHCl (Melts methods), which was

Table 1. Purity analysis result of TOAHCl by elemental analysis.

Sample	Elemental analysis (%)			
	C	H	N	Cl
Required	73.89	13.43	3.59	9.09
Synthesis	73.81	13.58	3.48	9.13

carried out on a Nicolet 6700 instrument (Thermo Fisher Scientific, USA). Thermal analysis methods such as TG, DSC, TG-DSC and TG-FTIR were also used to capture the mechanism of thermal dissociation process.

Dynamic thermogravimetric measurements (TG) were conducted on a PerkinElmer STA 6000 thermobalance which was coupled with a PerkinElmer FRONTIER FTIR spectrometer (PerkinElmer, USA). Samples weighing 8–10 mg were placed in a platinum crucible covered by a lid with a hole and heated at 10.0 K min^{-1} heating rate in a dynamic high purity N_2 atmosphere. Gaseous TG-FTIR result was the direct evidence for the dissociation mechanism.

Thermodynamics was determined by both TG and DSC methods which were realized on NETZSCH DSC 200F3 (NETZSCH, Germany). Samples weighing 6–10 mg were placed in a covered platinum crucible (the lid had a pinhole) and heated at 5 K min^{-1} and 10 K min^{-1} heating rate for DSC measurement. The dissociation process was better understood by analyzing the TG-DSC curves with the help of instrument NETZSCH STA 449F3 (NETZSCH, Germany). The platinum crucible was also covered by a lid with a pinhole. All were in a dynamic high purity N_2 atmosphere.

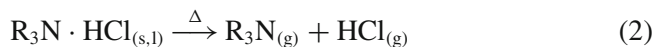
HWR-15C Automatic Calorimeter (Shanghai ANDE Instrument Equipment Co. Ltd) was used to calculate the enthalpy of formation of TOAHCl.

3. Results and Discussion

3.1 The reaction pathway determination

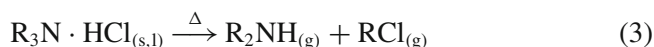
It has been suggested that amine hydrochlorides dissociate with the release of amines and HCl (both are

in gas phase).^{28–33} Therefore, the proposed dissociation process (pathway 1) can be described by the following equation:



where R stands for the hydrocarbon chain; in this paper, it is n-octyl.

Side reactions which produce secondary amines (pathway 2) even primary amines (not part of this paper) may occur at a higher temperature and for a longer time, resulting in the degradation of amines.³² As shown in the following equation.



Reaction mainly happens by the way of equation (2) because the N–H bond (more like an H-bonding) strength is weaker in comparison to that of the covalent C–N bond. Jerzy Blazejowski made the conclusion that there was a fairly high activation barrier for dealkylation based on the considerations of much higher dissociation enthalpies of quaternary salts than primary, secondary and tertiary amine hydrochlorides.³² However, there is no direct evidence for this explanation. Thus, we performed CI-NEB and IRC calculations to study the two possible pathways for the thermal dissociation of TOAHCl.

The results are shown in Figure 1. There is no barrier for the formation of TOA and HCl complex and the calculated reaction enthalpy value $69.395 \text{ kJ mol}^{-1}$ is consistent with the experimental studies hereinafter.

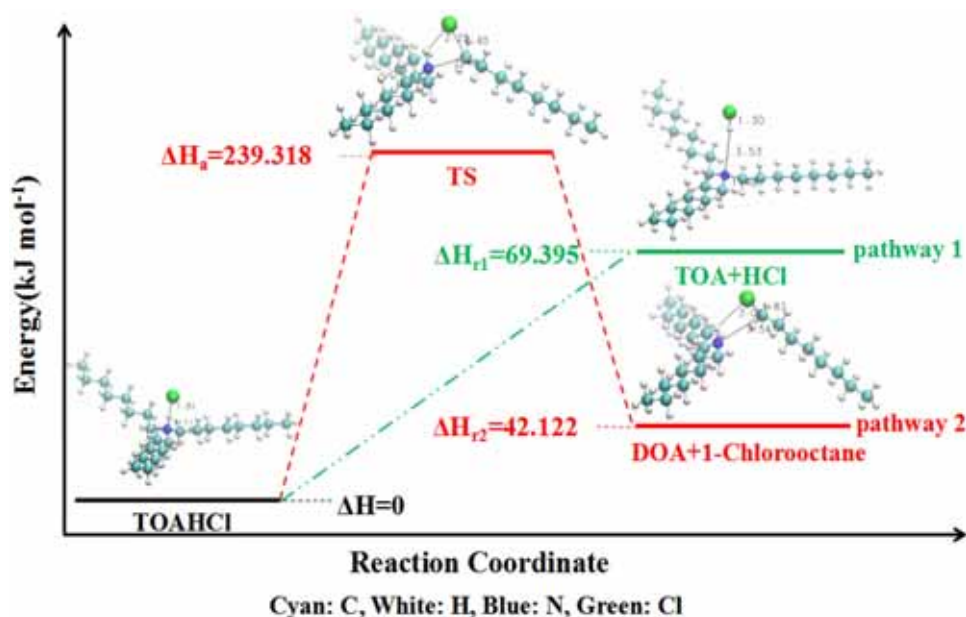


Figure 1. Two pathways for thermal dissociation of TOAHCl.

Whereas the reaction barrier is up to $239.318 \text{ kJ mol}^{-1}$ when forming DOA and 1-chlorooctane although the reaction enthalpy of pathway 2 valued $42.122 \text{ kJ mol}^{-1}$ is lower than that of pathway 1. Thus, we assume that TOAHCl mainly even only dissociates along pathway 1 under our experimental condition. It is also verified by the following experimental analysis. For the calculation details about IRC of pathway 2, total energy scanning of pathway 1 and others, please check Supplementary Information (SI).

3.2 Infrared spectra study on thermal dissociation

FTIR spectra of TOA and TOAHCl are compared⁴⁰ in Figure 2(a). When transformed to TOAHCl from TOA, the C–N stretch band at 1096 cm^{-1} shifts to 1050 cm^{-1} and its intensity becomes weaker. Then the Raman spectrum of TOAHCl was tested (shown in Figure 2(b)), which shows that the intensity of C–N out-of-phase stretch at about 1060 cm^{-1} is much stronger than that of IR. Moreover, C–N in-phase stretch at around 833 cm^{-1} appears which could hardly be found in IR spectra, indicating that C–N band tends to be Raman active after charge rearrangement (electrons cloud moved towards the center of C and N with inductive of Cl.) In other words, C–N becomes less polar than that in TOA even though the whole molecule TOAHCl becomes more polar. The frequency of CH_2 (next to N) in-phase stretch band at 2800 cm^{-1} increases to above 2900 cm^{-1} because of NH^+ group.⁴¹ Meanwhile, NH summation bands in the range between 2700 cm^{-1} and 2300 cm^{-1} appear. It should be pointed out that the band occurring at about 3400 cm^{-1} may belong to OH because of the sample making method or the trace water content in TOAHCl.

Jerzy Błazejowski pointed out that FTIR measurements coupled to thermogravimetric experiments (TG-FTIR) could be a reliable method for unambiguously identifying the species produced as a result of the thermal degradation of quaternary methylammonium or ethylammonium halides^{34,35} which could be applied to study the products of thermal dissociation of amine hydrochlorides.

The process of thermal dissociation of TOAHCl was monitored by recording FTIR spectra as a function of time. The “three-dimensional” FTIR spectrum of products (Figure 3(a)) displays that the intensities of the absorption signals pass through two successive maxima, which usually indicates the complex mechanism of this compound’s thermal dissociation. The same thing also happens in FTIR of TOA’s evaporation (Figure 3(b)), thus we could not make any further deduction from the simple two successive maxima in FTIR curve. On

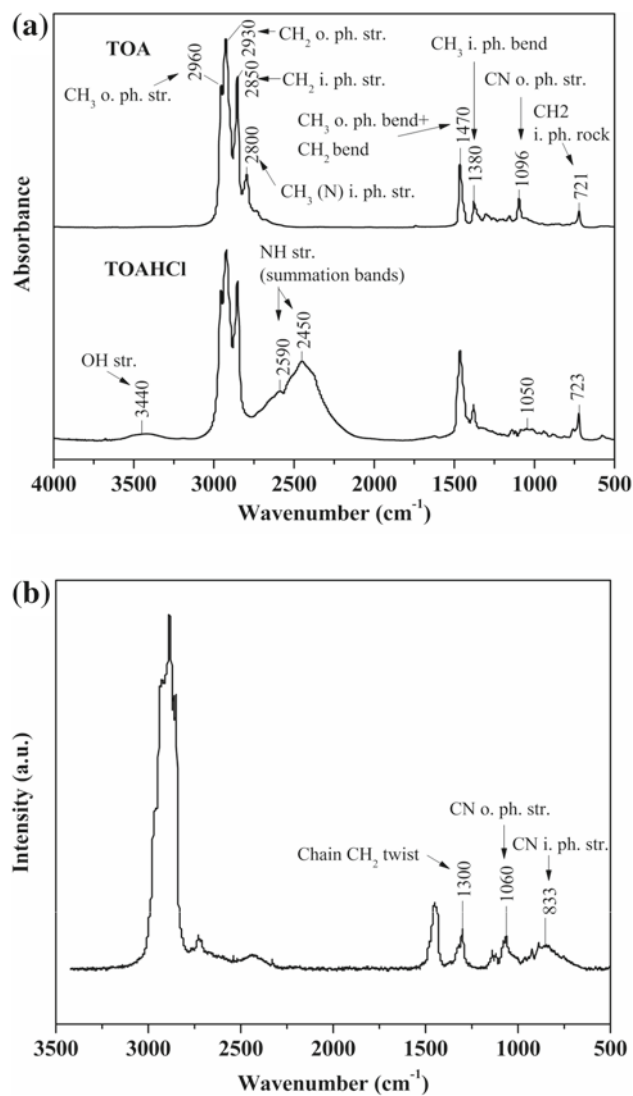


Figure 2. (a) FTIR spectra of TOA and TOAHCl; (b) Raman spectrum of TOAHCl.

the other hand, by analyzing the FTIR spectra at different times, some nuances can be found. The FTIR spectrum of TOA appears from the point of about 600 s (at about 140°C) to the end. Before around 1416 s (at about 283°C), FTIR spectra of a mixture of TOA and HCl ($3014\text{--}2700 \text{ cm}^{-1}$ summation bands^{42,43}) are shown whilst after 1460 s only FTIR spectra of TOA is recorded (Figure 4) except for the occasional very weak intensities of HCl compared to those before 1460 s. As is known, free HCl typically has a series of strong signatures from 3050 to 2650 cm^{-1} .⁴² Therefore, only weak signal appears mainly because HCl is not free molecule but bound by weak interaction with TOA, resulting in the masking of the HCl signal by those of TOA. In addition, during the period between 1596 s and 1673 s ($306\text{--}318.8^\circ\text{C}$), a peak of weak intensity at about 2711 cm^{-1} appears which is regarded as an

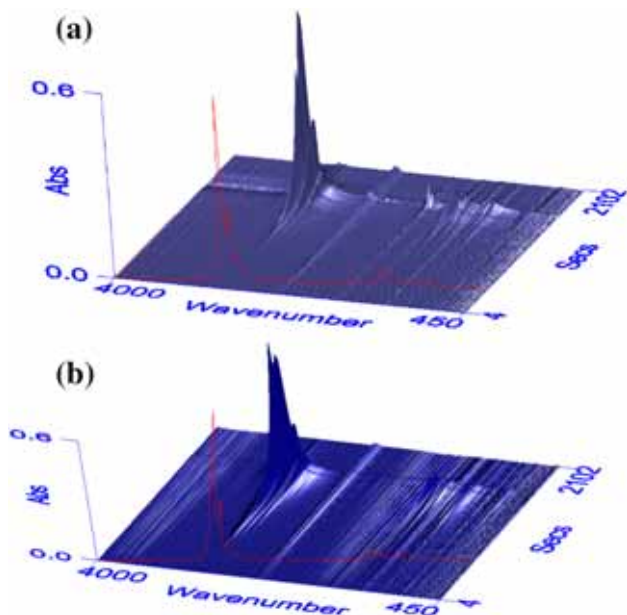


Figure 3. Time dependence of the FTIR spectra measured during the TG-FTIR experiments for TOAHCl (a) TOA (b).

implication of an intermediate form of TOA and HCl in gas phase, in which the proton is only partially transferred and shared by TOA and Cl^- .⁴⁴ In fact, the weak complexes between TOA and HCl ($\text{TOA} \cdots (\text{HCl})_n$) whose NH vibrations are weak can be expected on the basis of not only theoretical considerations^{44–46} but also certain experimental evidence^{47–50} for other kinds of amine hydrochlorides. Particularly, very useful infrared spectra data were analyzed in the references,^{49,50} pointing out signals around 630, 660, 672 cm^{-1} belonged to $\text{NH}_3 \cdot \text{HCl}$, $(\text{EtNH}_2)_2 \cdot \text{HCl}$ and $\text{NH}_3 \cdot (\text{HCl})_2$ complexes, respectively. The twin peaks at about 2360 cm^{-1} and 2340 cm^{-1} are believed to belong to CO_2 because of its existence all along. From the above analysis, some conclusions could be made. Firstly, the thermal dissociation of TOAHCl begins at about 140°C and starts to be evident at above 180°C. Secondly, the process is likely to be divided into two steps mainly due to the difference in evaporation rates. At lower temperatures, the release of HCl is faster than TOA due to the high boiling point of TOA (365°C), while at higher temperatures (above 275°C) the TOA and HCl escape from the system at about the same time once the dissociation happens. The side reactions mentioned in some references forming corresponding secondary or primary amine and chlorinated hydrocarbon⁵¹ did not happen in the experiment (there is no strong intensity at about 725 as well as 655 cm^{-1} which belong to C–Cl bond⁴⁰) because of the short time of heating and the lower temperature. The result is consistent with the DFT calculations.

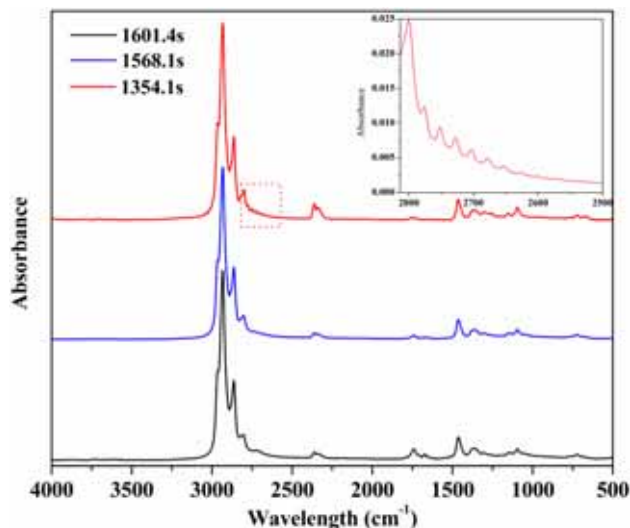


Figure 4. FTIR spectra of the products of TOAHCl at 1354.1 s, 1568.1 s and 1601.4 s (about 266°C and 301°C, 306.9°C, accordingly).

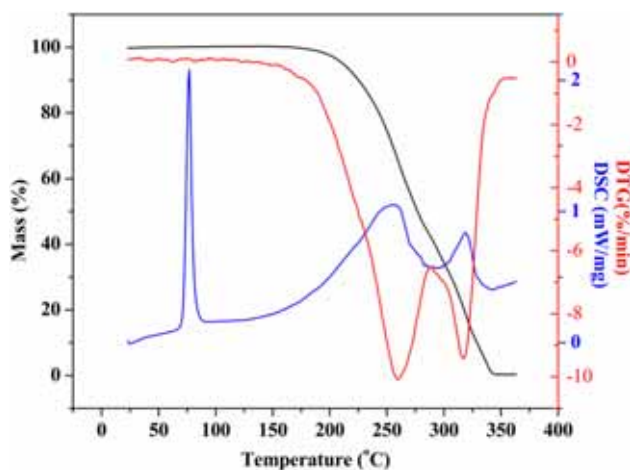


Figure 5. TG/DSC/DTG curves of the thermal dissociation process of TOAHCl.

3.3 Thermal analysis of thermal dissociation

With the aid of NETZSCH STA 449F3, TG/DSC/DTG curves of the thermal dissociation process of TOAHCl are depicted as Figure 5. We can see from the picture that the dissociation process is obviously divided into two steps, and both are endothermic. Before the temperature about 287°C, the mass loss was 57% while the rest is 43%. The result also demonstrates that HCl and TOA do not release separately. (if the whole HCl release before TOA evaporation then the first step mass loss should be around 9.35%). The specific reason why it happens like this is still not very clear so far. The evaporation rates might matter.

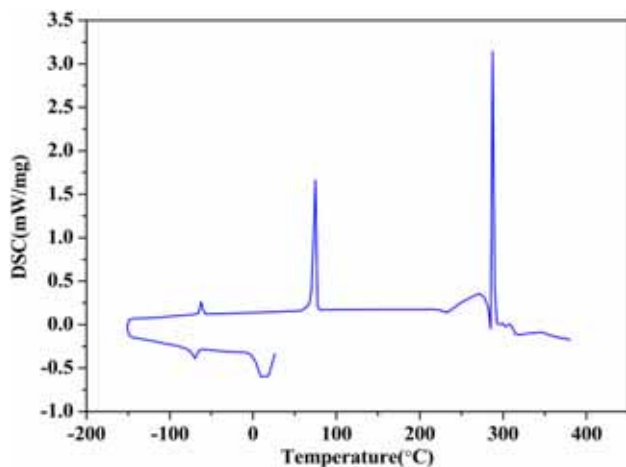


Figure 6. DSC result of TOAHCl at heating rate of 5 K min⁻¹.

In this paper, complete DSC curves were obtained with the help of liquid nitrogen. We can see from Figure 6 that polymorphic transformation appears at -62°C and the enthalpy is 2.467 kJ mol⁻¹. Melting with the enthalpy of 27.735 kJ mol⁻¹ happens before dissociation process at about 73°C. The thermal dissociation process begins at about 240°C and ends at about 287°C, which experiences two successive stages, with a chunky peak first and a sharp one then. The enthalpies are 70.427 kJ mol⁻¹ and 71.158 kJ mol⁻¹ for 5 K min⁻¹ (Figure 6) and 10 K min⁻¹ (Figure 7), respectively which are very close to the DFT calculation values 69.395 kJ mol⁻¹. However, the enthalpies of the second stage occupy 50% and 71.6% of the totals. This phenomenon may be explained with the result of TG-FTIR spectra. At lower temperatures, the release speed of HCl is much higher than that of TOA and TOA is believed to inhibit the process of dissociation, thus a chunky peak appeared. While at higher temperatures, TOA emits together with HCl once the dissociation process happens, and the vaporization of TOA is the main part of the enthalpy, thereby forming a sharp peak at the second stage. Due to doubled heating rates at two separate tests, the second stage enthalpy of 10 K min⁻¹ is much larger than that of 5 K min⁻¹. What should be noted is that the starting temperatures from Figures 6, 7 are much higher than that from TG-FTIR result, mainly due to the size of the hole in the lid. The size is larger in the latter experiment, thus the thermodynamically controlled reaction⁴² happens at a lower temperature.

3.4 Thermodynamics of thermal dissociation process

3.4a Calculation of enthalpy of thermal dissociation: Calculation of some important thermodynamic

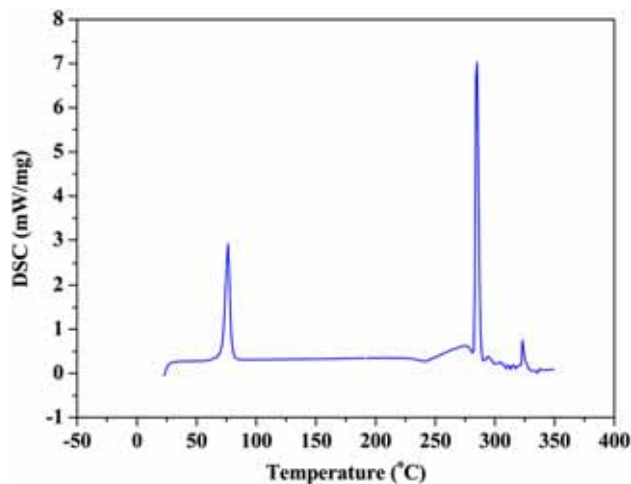


Figure 7. DSC result of TOAHCl at heating rate of 10 K min⁻¹.

parameters such as enthalpy through experimental and molecular simulation methods or their combination is of great importance to make a thorough study on the thermal dissociation process.

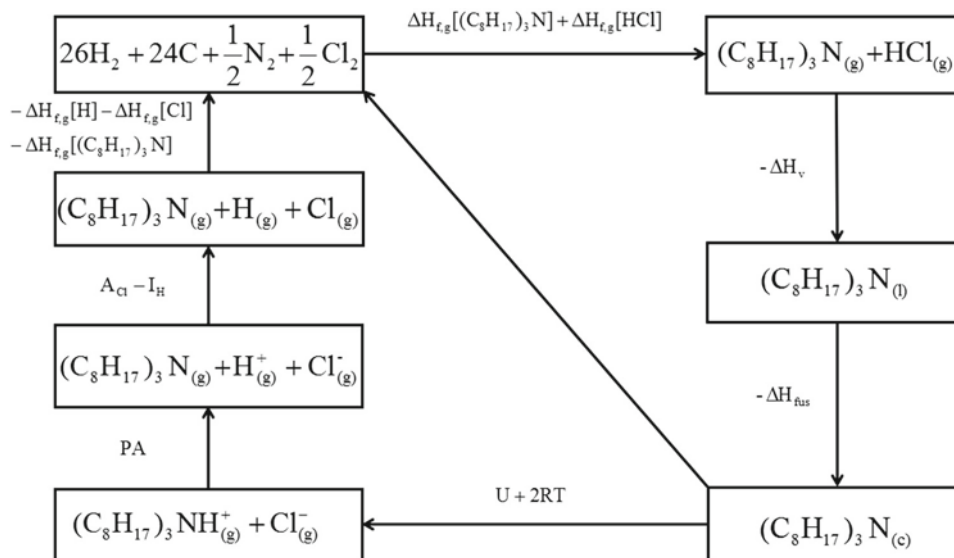
Enthalpies of thermal dissociation are usually estimated by fitting the thermogravimetric traces to the Van't Hoff equation:^{2,23-25}

$$\ln \alpha = -\frac{\Delta_d H^0}{2R} \frac{1}{T} + \frac{\Delta_d H^0}{2R} \frac{1}{T_d} \quad (4)$$

where α represents the degree of the reaction, T_d is the temperature at which α equals 1, and R is the gas constant, 8.3145 J K⁻¹ mol⁻¹. By this method, the enthalpy of dissociation was evaluated with the value of 188.297 kJ mol⁻¹. The primary premise of this method is that the system achieves equilibrium at given temperatures, which indicates that the only energy barrier existing for the process is the thermodynamics one, *i.e.*, $\Delta_v H^0$.³⁴ However, it is not satisfied with the premise because of the open crucible with a dynamic nitrogen atmosphere. Thus, enthalpy of thermal dissociation of TOAHCl obtained with DSC measurement is a better choice. The value 70.793 kJ mol⁻¹ is very close to the enthalpy of vaporization of TOA at 600 K/between 505 K and 702 K, 71.5 ± 7.6/70.6 kJ mol⁻¹,⁵¹ showing that enthalpy of vaporization of TOA is the main part of enthalpy of dissociation. It is known that the value for the enthalpy of dissociation does not refer to 298.15 K. Thus, a modification is necessary.

$$\Delta H_{v,298}^0 = \Delta H_v^0 + \Delta H_{fn}^0 + \sum \Delta H_{\sigma}^0 - \int_{298}^T \Delta C_p^0 dT \quad (5)$$

where ΔH_{fn}^0 refers to the enthalpy of fusion, 29.954 kJ mol⁻¹ in this work. The term $\sum \Delta H_{\sigma}^0$ arises from polymorphic transitions that the salts may experience



Scheme 1. The extended Born–Fajans–Haber cycle for TOAHCl.

between 298.15 K and the beginning of the fusion or dissociation process. For TOAHCl, this term equals to 0. The heat capacity term is equal to 7.0 kJ mol^{-1} ²⁹ which was considered the same as NH_4Cl .²⁹ Thus, the derived value of the dissociation of TOAHCl is $107.747 \text{ kJ mol}^{-1}$, which is quite close to the enthalpy of vaporization of TOA at 298.15 K, $110.4 \pm 15.0 \text{ kJ mol}^{-1}$,⁵¹ demonstrating the vaporization of TOA is the controlling step for the dissociation reaction

3.4b Evaluation of other important thermochemical characteristics: Numerous thermochemical quantities for ionic crystals can be derived from a simple Hess's law. The relationships between these properties could be described in the form of a thermochemical cycle known as Born–Fajans–Haber cycle.^{52,53} The thermochemical characteristics of TOAHCl could be calculated with such a cycle (Scheme 1).

3.4c Enthalpy of formation of $[(\text{C}_8\text{H}_{17})_3\text{NH}]\text{Cl}$:

The value of $\Delta H_{f,c}^0$ for $[(\text{C}_8\text{H}_{17})_3\text{NH}]\text{Cl}$ can be calculated according to the equation below from the thermochemical cycle mentioned above.

$$\Delta H_{f,c}^0[(\text{C}_8\text{H}_{17})_3\text{NHCl}] = \Delta H_{f,c}^0[(\text{C}_8\text{H}_{17})_3\text{N}] + \Delta H_{f,c}^0[\text{HCl}] - \Delta H_{\text{fus}}^0 - \Delta H_{\text{v}}^0 \quad (6)$$

The values of ΔH_{fus}^0 and ΔH_{v}^0 are $29.954 \text{ kJ mol}^{-1}$ and $107.747 \text{ kJ mol}^{-1}$ which were obtained in this paper. Values for $\Delta H_{f,g}^0[(\text{C}_8\text{H}_{17})_3\text{N}]$ and $\Delta H_{f,g}^0[\text{HCl}]$ equal to $-477.100 \text{ kJ mol}^{-1}$ ⁵¹ and $-92.300 \text{ kJ mol}^{-1}$.^{29,54} Thus, the value of $\Delta H_{f,g}^0[(\text{C}_8\text{H}_{17})_3\text{NHCl}]$ is $-707.101 \text{ kJ mol}^{-1}$ with DSC method while it is -694.673

kJ mol^{-1} using calorimetric method, which is almost the same.

3.4d Crystal lattice energy of $[(\text{C}_8\text{H}_{17})_3\text{NH}]\text{Cl}$: From the thermochemical cycle presented in Scheme 1, the following independent relations may be derived.

$$U^0 + 2RT + PA - I_{\text{H}} + A_{\text{Cl}} + \Delta H_{f,g}^0[\text{HCl}] - \Delta H_{f,g}^0[\text{H}] - \Delta H_{f,g}^0[\text{Cl}] - \Delta H_{f,g}^0[(\text{C}_8\text{H}_{17})_3\text{N}] + \Delta H_{f,g}^0[(\text{C}_8\text{H}_{17})_3\text{N}] - \Delta H_{\text{v}}^0 - \Delta H_{\text{fus}}^0 = 0 \quad (7)$$

Since

$$\Delta H_{f,g}^0[\text{H}^+] = \Delta H_{f,g}^0[\text{H}] + I_{\text{H}} \quad (8)$$

and

$$\Delta H_{f,g}^0[\text{Cl}^-] = \Delta H_{f,g}^0[\text{Cl}] - A_{\text{Cl}} \quad (9)$$

Equation (7) may be rearranged to the form.

$$U^0 = -PA - 2RT + \Delta H_{f,g}^0[\text{H}^+] + \Delta H_{f,g}^0[\text{Cl}^-] - \Delta H_{f,g}^0[\text{HCl}] + \Delta H_{\text{v}}^0 + \Delta H_{\text{fus}}^0 \quad (10)$$

where PA denotes the proton affinity of appropriate amines, *i.e.*, the negative values of the enthalpy of reaction (10),⁵⁵ which was calculated with Gaussian09, at B3LYP/6-311++G(d,p) level. The value of PA is $1014.559 \text{ kJ mol}^{-1}$.



Thus the crystal energy of TOAHCl is $510.597 \text{ kJ mol}^{-1}$, which is dependable according to Jerzy Błazewski's statements.³²

4. Conclusions

High purity solid TOAHCl was prepared and certified by elementary analysis. The two possible dissociation pathways of TOAHCl were studied by DFT calculations and confirmed by performing IRC. Although the enthalpy of the reaction pathway 1 is higher than that of pathway 2 (69.395 and 42.122 kJ mol⁻¹, respectively), there is no barrier for HCl leaving in pathway 1 whereas there is a fairly high activation barrier of 239.318 kJ mol⁻¹ for dealkylation pathway. Therefore, the former should be the dominant pathway which is consistent with the experimental findings.

The thermal dissociation of the compound was analyzed using TG, DSC, FTIR techniques. Through DSC and TG-DSC experiments, two successive steps appear during the thermal dissociation of TOAHCl. It could be explained that at lower temperatures (from about 140°C), the dissociation began with the escape of more HCl than TOA. It shows a broad and blunt endothermic peak because TOA inhibited the dissociation process. Then the process of release of both TOA and HCl or even just the TOA at higher temperature happens during which time a sharp endothermic peak is formed. In addition, enthalpy of vaporization of TOA was found to be the main source of the entire enthalpy of dissociation. FTIR spectra tell us that after an initial increase, the absorption signal passes through two successive maxima and then gradually decreases. All the FTIR absorption bands behave almost in the same manner, suggesting that the relevant products are formed from the onset of dissociation till the end of this process. The strong agreement between the experimental FTIR spectra and those of standard samples demonstrates directly for the first time that a mixture of TOA and HCl is produced as a result of dissociation.

For kinetics of this process, this paper did not discuss because most models are applied under the condition of solid reactant, but for us, it is the liquid TOAHCl that dissociates. Also, the specific reasons and evidence for the occurrence of two steps in dissociation process need further consideration. We are trying to search for the proper methods.

Supplementary Information (SI)

Structures of reactants, products, transition state, figures with characteristic bond lengths along the reaction paths, energy profiles along the reaction coordinates of pathway 1 and IRC calculations for pathway 2, input files for searching TS, vibrational frequencies of transition state and confirmation with IRC are provided in

Supplementary Information, which is available at www.ias.ac.in/chemsci.

Acknowledgements

The authors are greatly thankful to the National High Technology Research and Development Program of China (No. 2011AA06A107) for financial support. Also, authors thank China Scholarship Council (CSC) for backing the project. Authors thank the University of Amsterdam and SURFsara in The Netherlands for offering the resources for calculation on CP2K and Gaussian 09, respectively.

References

- Sarangi K, Padhan E, Sarma P V R B, Park K H and Das R P 2006 Removal/recovery of hydrochloric acid using Alamine 336, Aliquat 336, TBP and Cyanex 923 *Hydrometallurgy* **84** 125
- Kojima T, Fukutomi H and Kakihana H 1969 Extraction of hydrochloric acid by tri-n-octylamine in benzene *B. Chem. Soc. Jpn.* **42** 875
- Schunk A and Maurer G 2003 Distribution of hydrochloric, nitric, and sulfuric acids between water and organic solutions of tri-n-octylamine Part I. Toluene as organic solvent *Fluid Phase Equilibria* **207** 1
- Schunk A and Maurer G 2003 Distribution of hydrochloric, nitric, and sulfuric acids between water and organic solutions of tri-n-octylamine Part II. Methylisobutylketone as organic solvent *Fluid Phase Equilibria* **21** 189
- Agrawal A and Sahu K K 2009 An overview of the recovery of acid from spent acidic solutions from steel and electroplating industries *J. Hazard. Mater.* **171** 61
- Nguyen T H and Lee M S 2014 Extraction and stripping of inorganic acids by tris-2-ethylhexyl amine *J. Korean Inst. Met. Mater.* **52** 799
- Banda R, Nguyen T H, Sohn S H and Lee M S 2013 Recovery of valuable metals and regeneration of acid from the leaching solution of spent HDS catalysts by solvent extraction *Hydrometallurgy* **133** 161
- Banda R, Nguyen T H and Lee M S 2013 Recovery of HCl from chloride leach solution of spent HDS catalyst by solvent extraction *Chem. Process Eng.* **34** 153
- Fu X, Liu H, Chen H, Hu Z and Wang D 1999 Three-phase extraction study of the TOA-alkane/HCl (Zn²⁺ or Fe³⁺) systems *Solv. Extr. Ion. Exch.* **17** 1281
- Li Y, Song X, Chen G, Sun S, Xu Y and Yu J 2015 Extraction of hydrogen chloride by a coupled reaction-solvent extraction process *Front. Chem. Sci. Eng.* **9** 479
- Li Y, Song X, Chen G, Sun Z, Xu Y and Yu J 2015 Preparation of calcium carbonate and hydrogen chloride from distiller waste based on reactive extraction-crystallization process *Chem. Eng. J.* **278** 55
- Liu X, Wang W, Wang M and Wang P 2014 Experimental Study of CO₂ mineralization in Ca²⁺-rich aqueous using tributylamine as an enhancing medium *Energ. Fuel.* **28** 2047

13. Wang W, Liu X, Wang P, Zheng Y and Wang M 2013 Enhancement of CO₂ mineralization in Ca²⁺-/Mg²⁺-rich aqueous solutions using insoluble amine *Ind. Eng. Chem. Res.* **52** 8028
14. Chen G, Song X, Dong C, Sun S, Sun Z and Yu J 2016 Mineralizing CO₂ as MgCO₃ · 3H₂O Using Abandoned MgCl₂ Based on a Coupled Reaction–Extraction–Alcohol Precipitation Process *Energ. Fuel.* **30** 7551
15. Xu X and Zhu T 2005 Coupled process of reaction and solvent extraction I. The reaction between CO₂ and SrCl₂ coupled with solvent extraction of HCl *Hydrometallurgy* **76** 11
16. Zhou Z, Liang F, Qin W and Fei W 2014 Coupled reaction and solvent extraction process to form Li₂CO₃: mechanism and product characterization *AIChE J.* **60** 282
17. Agrawal A 2007 Extraction of acid and iron values from sulphate waste pickle liquor of a steel industry by solvent extraction route *Hydrometallurgy* **88** 55
18. Huang Q, Jin F, and Kang S 2007 Production of potash by amine extraction *Chem. Ind. Eng.* **24** 304 (in Chinese)
19. Kang H, Zhou X, Dong L and Feng T 2011 Synergetic extraction of phytic acid from HCl extract of rapeseed meal with Alamine 336 and n-octanol dissolved in sulfonated kerosene *Ind. Eng. Chem. Res.* **50** 8658
20. Eyal A and Banlél A 1982 Extraction of strong mineral acids by organic acid-base couples *Ind. Eng. Chem. Proc. Dd.* **21** 334
21. Zhang J, Zhang R, Geerlings H and Bi J 2010 A novel indirect wollastonite carbonation route for CO₂ sequestration *Chem. Eng. Technol.* **33** 1177
22. Coenen A, Kosswig K and Prominski G 1978 *Process for obtaining gaseous hydrogen chloride from dilute, aqueous hydrochloric acid* U.S. Patent 4115530
23. Coenen A, Kosswig K, Hentschel B and Ziebarth J 1980 *Method of manufacturing hydrogen chloride from solutions of amine hydrochlorides* U.S. Patent 4230681
24. Eyal A M and Baniel A M 1991 Recovery and concentration of strong mineral acids from dilute solutions through LLX. I. Review of parameters for adjusting extractant properties and analysis of process options *Solvent Extr. Ion Exc.* **9** 195
25. Hentschel B, Ziebarth J, Coenen A, Kosswig K and Praun F V 1982 *Method for preparing sodium bicarbonate and hydrogen chloride* U.S. Patent 4337234
26. Baniel A and Eyal A 2010 *Process for the recovery of HCl from a dilute solution thereof* U.S. Patent 2010/0093995 A1
27. Baniel A and Eyal A 2011 *Process for the recovery of HCl from a dilute solution thereof and extractant composition for use therein* U.S. Patent 2011/0028710 A1
28. Błażejowski J, Szychliński J and Kowalewska E 1993 Thermal reactions of lead(IV) chloride complexes in the solid state. Part V. Thermolysis of mono-n-alkylammonium hexachloroplumbates *Thermochim. Acta* **66** 197
29. Błażejowski J 1983 Thermal properties of amine hydrochlorides. Part I. Thermolysis of primary n-alkylammonium chlorides *Thermochim. Acta* **68** 233
30. Rodebush W H and Michalek J C 1929 The vapor pressure and vapor density of intensively dried ammonium chloride *J. Am. Chem. Soc.* **51** 748
31. Harrison R M, Sturges W T, Kitto A M N and Li Y 1990 Kinetics of evaporation of ammonium chloride and ammonium nitrate aerosols *Atmos. Environ.* **24A** 1883
32. Błażejowski J and Kowalewska E 1986 Thermal properties of amine hydrochlorides. Part II. Thermolysis and thermochemistry of alkanaminium chlorides *Thermochim. Acta* **105** 257
33. Błażejowski J, Krzymiński K, Storiński P and Rak J 2000 Thermodynamics and kinetics of the thermal decomposition of N,N,N-Trimethylmethanaminium and 1-Methylpyridinium halides *J. Therm. Anal. Calorim.* **60** 927
34. Sawicka M, Błażejowski J and Rak J 2006 TG-FTIR, DSC and quantum chemical studies of the thermal decomposition of quaternary methylammonium halides *Chem. Phys.* **324** 425
35. Sawicka M, Błażejowski J and Rak J 2006 TG-FTIR, DSC, and quantum-chemical studies on the thermal decomposition of quaternary ethylammonium halides *J. Phys. Chem. A* **110** 5066
36. Mills G and Jónsson H 1994 Quantum and thermal effects in H₂ dissociative adsorption: Evaluation of free energy barriers in multidimensional quantum systems *Phys. Rev. Lett.* **72** 1124
37. Henkelman G and Jónsson H 2000 Improved tangent estimate in the nudged elastic band method for finding minimum energy paths and saddle points *J. Chem. Phys.* **113** 9978
38. Hutter J Iannuzzi M Schiffmann F and Vondel J V 2014 *WIRES Comput. Mol. Sci.* **4** 15
39. Frisch M J, Trucks G W, Schlegel H B, et al. Gaussian 09, revision D.01; Gaussian, Inc.: Wallingford CT, 2009.
40. Larkin P J 2011 In *Infrared and Raman Spectroscopy: Principles and Spectral Interpretation* P J Larkin (Ed.) (Elsevier Inc.: Waltham MA) p. 75, 76, 78, 107, 109, 120, 126, 157, 158
41. Weng S In *Fourier transform infrared spectrum* 2nd edn. J X Du and D Xiang (Ed.) (Chemical Industry Press: Beijing) p. 338 (in Chinese)
42. Gibson E K 2007 Amine hydrochloride salts: a problem in polyurethane synthesis (University of Glasgow, Glasgow, UK) pp. 98–100, 103
43. Bauer S H, Yamazaki T, Lazaar K I and Chiu N S 1985 Intermolecular conversion over a low barrier. 3. Gas-phase NMR studies of an H bond association *J. Am. Chem. Soc.* **107** 743
44. Latajka Z, Sakai S and Morokuma K 1984 Possible gas-phase ion pairs in amine-HCl complexes. An ab initio theoretical study *Chem. Phys. Lett.* **110** 464
45. Clementi E and Gayles J N 1967 Study of the Electronic Structure of Molecules. VII. Inner and Outer Complex in the NH₄Cl Formation from NH₃ and HCl *J. Chem. Phys.* **47** 3837
46. Brciz A, Karpfen A, Lischka H and Schuster P 1984 A candidate for an ion pair in the vapor phase: Proton transfer in complexes R₃N-HX *Chem. Phys.* **89** 337
47. Goldfinger P and Verhaegen G 1969 Stability of the gaseous ammonium chloride molecule *J. Chem. Phys.* **50** 1467

48. de Kruif G G 1982 The vapor phase dissociation of ammonium salts: Ammonium halides, ammonium rhodanide, ammonium nitrate, and ammonium bicarbonate *J. Chem. Phys.* **77** 6247
49. Barnes A J, Beech T R and Mielke Z 1984 Strongly hydrogen-bonded molecular complexes studied by matrix-isolation vibrational spectroscopy Part 1. The ammonia-hydrogen chloride complex *J. Chem. Soc., Faraday Trans. 2* **80** 455
50. Barnes A J, Nicholas J, Kuzniarski S and Mielke Z 1984 Strongly hydrogen-bonded molecular complexes studied by matrix-isolation vibrational spectroscopy Part 2. Amine-hydrogen chloride complex *J. Chem. Soc., Faraday Trans. 2* **80** 465
51. Steele W V, Chirico R D, Knipmeyer S E, Nguyen A, Smith N K and Tasker I R 1996 Thermodynamic properties and ideal-gas enthalpies of formation for cyclohexene, phthalan (2,5-Dihydrobenzo-3,4-furan), isoxazole, octylamine, dioctylamine, trioctylamine, phenyl isocyanate, and 1,4,5,6-tetrahydropyrimidine *J. Chem. Eng. Data* **41** 1269
52. Waddington T C 1959 Lattice energies and their significance in inorganic chemistry *Adv. Inorg. Chem. Radiochem.* **1** 157
53. Goodliffe A L, Jenkins H D B and Martin S V 1971 The proton affinity of gaseous ammonia, the charge distribution on the NH_4^+ ion and the lattice energies of NH_4Cl , NH_4Br and NH_4I *Mol. Phys.* **21** 761
54. Lide D R 2004 In *CRC Handbook of Chemistry and Physics* 85th edn. D R Lide (Ed.) (London: CRC press) pp. 5-2
55. Valadbeigi Y, Farrokhpour H and Tabrizchi M 2014 G4MP2, DFT and CBS-Q calculation of proton and electron affinities, gas phase basicities and ionization energies of hydroxylamines and alkanolamines *J. Chem. Sci.* **126** 1209